View metadata, citation and similar papers at core.ac.uk
brought to you by CORE
provided by RERO DOC Digital Library

Histochem Cell Biol (2007) 128:161–173
DOI 10.1007/s00418-007-0304-8

ORIGINAL PAPER

Expression of mutant Ins2^{C96Y} results in enhanced tubule formation causing enlargement of pre-Golgi intermediates of CHO cells

Jing-Yu Fan · Jürgen Roth · Christian Zuber

Accepted: 8 June 2007 / Published online: 24 July 2007
© Springer-Verlag 2007

Abstract Misfolded proteins are recognized by the protein quality control and eventually degraded by the ubiquitin-proteasome system. Previously, we demonstrated accumulation of a misfolded non-glycosylated protein, namely proinsulin, in enlarged pre-Golgi intermediates and dilated rough endoplasmic reticulum (ER) domains in pancreatic β-cells of Akita mice. In order to exclude effects possibly due to coexisting wild type and mutant proinsulin in pancreatic β-cells, CHO cells expressing singly wild type or mutant C96Y proinsulin 2 were now analyzed by electron microscopic morphometry and immunogold labeling as well as serial section 3D analysis. We found a significant increase in volume density of pre-Golgi intermediates in CHO Ins2^{C96Y} cells which was principally due to an increase of its tubular elements, and no significant changes of the ER. The average diameter of the pre-Golgi intermediates of CHO Ins2^{C96Y} cells was about twice that of CHO Ins2^{wt} cells. The enlarged pre-Golgi intermediates and the ER of CHO Ins2^{C96Y} cells were positive for proinsulin, which was not detectable in the significantly enlarged Golgi cisternal stack. Treatment of CHO Ins2^{C96Y} cells with proteasome inhibitors resulted in the formation of proinsulin-containing aggresomes. We conclude that misfolded proinsulin causes enlargement of pre-Golgi intermediates which indicates their involvement in protein quality control.

Keywords Proinsulin · Pre-Golgi intermediates · Endoplasmic reticulum · Protein quality control · Morphometry

J.-Y. Fan · J. Roth · C. Zuber (✉)
Division of Cell and Molecular Pathology,
Department of Pathology, University of Zürich,
CH-8091 Zürich, Switzerland
e-mail: christian.zuber@usz.ch

Introduction

During synthesis and subsequent traffic, proteins are surveyed by a system of quality control which monitors their folding and assembly state and eliminates faulty products (Ellgaard and Helenius 2003; Meusser et al. 2005; Roth 2002; Sitia and Braakman 2003). It is noteworthy that folding of de novo synthesized proteins, despite the assistance of chaperones, is an inefficient process yielding often <50% mature proteins suited for transport beyond the endoplasmic reticulum (ER) (Lukacs et al. 1994; Petäjä-Repo et al. 2000; Ward and Kopito 1994). Nonetheless, the high rate of protein waste production appears not to be harmful to cells. The situation strikingly changes when proteins permanently fail to fold due to mutations or chronic stress. In fact, many congenital diseases have been recognized to be due to protein misfolding (Aridor and Hannan 2002; Barral et al. 2004; Kim and Arvan 1998). However, morphological signs of cellular indigestion and of cell injury may be variable in the various protein folding diseases. The ER and the pre-Golgi intermediates can appear structurally unaltered when misfolded proteins are efficiently degraded by the proteasome (Hirano et al. 2003; Naim et al. 1988; Tamarappoo and Verkman 1998; Yam et al. 2006). On the other hand, accumulation of misfolded proteins may cause distention of ER cisternae and enlargement of pre-Golgi intermediates (Gilbert et al. 1998; MedeirosNeto et al. 1996; Raposo et al. 1995; Zuber et al. 2004). Different types of inclusion bodies represent other structural hallmarks of protein folding diseases. For instance, Russell bodies, which are distended parts of ER, arise from the accumulation of insoluble aggregates of misfolded proteins (Alanen et al. 1985; Kopito and Sitia 2000; Mattioli et al. 2006; Valetti et al. 1991; Yam et al. 2007). On the other hand, aggresomes represent pericentriolar cytosolic accumulations of aggregated proteins, which form when the

digestive capacity of the proteasome is exceeded or its proteolytic activity is experimentally inhibited (Fabunmi et al. 2000; Garcia-Mata et al. 2002; Johnston et al. 1998; Kopito and Sitia 2000; McNaught et al. 2002; Wigley et al. 1999; Wojcik et al. 1996; Zatloukal et al. 2002).

Akita mice represents an animal model for type 2 diabetes (Kayo and Koizumi 1998; Yoshioka et al. 1997). The animals are heterozygous for a missense mutation in the insulin 2 gene that substitutes tyrosine for cystein at position 96 and disrupts one of the two disulfide bounds between the A and B chain of proinsulin (Wang et al. 1999). The mutant, non-convertable proinsulin ($Ins2^{C96Y}$) in pancreatic β-cells, as well as in transfected CHO cells, has been shown to accumulate intracellularly as dimers or higher molecular mass forms, to cause overexpression of BiP and PDI, and to form complexes with BiP (Oyadomari et al. 2002b; Wang et al. 1999). Although the mutant $Ins2^{C96Y}$ becomes degraded by the ubiquitin-proteasome pathway, it also induced ER stress markers and components of the ER-associated protein degradation (ERAD) (Allen et al. 2004). ER stress, therefore, is a major pathogenetic factor in β-cell apoptosis (Harding and Ron 2002; Oyadomari et al. 2002a) and has been shown to be causative for the development of diabetes in Akita mice (Oyadomari et al. 2002b).

Our previous analysis by electron microscopic morphometry, serial section analysis, and immunoelectron microscopy of pancreatic β-cells of Akita mice demonstrated accumulation of proinsulin mainly in expanded pre-Golgi intermediates and to a lesser extent in dilated ER subdomains (Zuber et al. 2004). A prominent feature of the expanded pre-Golgi intermediates were tubules with an average diameter of 102 nm and a length of up to 500 nm. Tubules of the same dimensions existed in the pre-Golgi intermediates of β-cells of control mice (Fan et al. 2003). However, their number was significantly increased in Akita mice β-cells. These studies have provided insight into the cellular and molecular pathology of this animal model of a protein folding disease.

In the present study, CHO cells stably expressing singly wild type proinsulin 2 ($Ins2^{wt}$) or mutant $Ins2^{C96Y}$ were investigated. We analyzed the early secretory pathway of the transfected CHO cells by electron microscopic morphometry, 3D reconstruction from serial ultrathin sections and immunogold electron microscopy. Furthermore, the effect of proteasome inhibition was analyzed.

Materials and methods

Reagents

Mouse monoclonal anti-human proinsulin antibodies were a gift of Dr. O. Madsen (Madsen et al. 1984), mouse monoclonal anti-ERGIC-53 (clone G1/93) antibodies a gift of Dr. H.-P. Hauri (Schweizer et al. 1988) and rabbit anti-β COP antibodies were kindly provided by Dr. R. Pepperkok (Pepperkok et al. 1993). Guinea pig anti-rat C-peptide antibody was purchased from Linco Research Inc., St. Charles, MI, USA, affinity-purified rabbit anti-mouse IgG, goat anti-mouse IgG and goat anti-rabbit IgG antibodies as well as RedX-conjugated Fab goat anti-mouse IgG from Jackson ImmunoResearch Laboratories Inc., West Grove, PA, USA, and Alexa488-conjugated goat anti-guinea pig IgG from Invitrogen, Carlsbad, CA, USA. Staphylococcal protein A (Pharmacia, Kalamazoo, MI, USA) was complexed with 8 nm gold particles (Roth et al. 1978) and affinity-purified secondary antibodies with 6 or 12 nm gold particles (Lucocq and Baschong 1986). Lactacystin was purchased from Sigma, Buchs, Switzerland, MG 132 from Calbiochem, VWR, Dietikon, Switzerland, and low melting Agar from FMC Bioproducts, Rockland, ME, USA. CHO cells stably expressing wild type (clone w22) or mutant $Ins2^{C96Y}$ (clone a7) were kindly provided by Dr. T. Izumi (Wang et al. 1999). The cells were cultured in F12 medium supplemented with 10% fetal calf serum.

Electron microscopic morphometry

Monolayer cultures of CHO cells were fixed in situ with a mixture of 2% paraformaldehyde and 0.1% glutaraldehyde in PBS (10 mM phosphate buffer, pH 7.4, and 0.15 M NaCl) for 30 min at initially 37°C, and post-fixed with 1% aqueous OsO_4 for 1 h at ambient temperature. Cells were removed with a rubber policeman, sedimented by centrifugation, enclosed in 2% low melting Agarose and embedded in Epon according to standard protocol. In order to study the effect of proteasome inhibition, cell cultures were grown in the presence of lactacystin (50 μM) for 2 and 4 h or MG 132 (20 μM) for 6 h and fixed as described above followed by Epon embedding.

For each CHO cell line, thin sections (70 nm nominal thickness) were cut from three different blocks and 20 photographs each were taken at an original magnification of ×8,000. Negatives were scanned using Adobe Photoshop® software and enlarged to a final magnification of ×27,700. Measurement of organelle volume density (V_v) and numerical density on area (N_A, which is the number of profiles per unit area of reference structure) were carried out by using the point counting method (Weibel 1979). For the point counting, the digitized electron micrographs were overlaid with a grid having a line spacing of 1.73 cm corresponding to 0.62 μm on the electron micrograph. Since the reference area, the cytoplasm, varied from photograph to photograph, the weighted average of V_V and N_A had to be calculated. The following equations were used to

calculate the average (M) and the square of standard deviation (SD^2).

$$M = \frac{\sum X_i}{\sum P_i},$$

and

$$SD^2 = \frac{n^2}{(n-1)\left(\sum P_i\right)^2} \times \left\{\sum X_i^2 + M \sum P_i^2 - 2M \sum P_i X_i\right\}.$$

X_i: points over the structure of interest; P_i: points over the reference area (cytoplasm); n: number of photographs evaluated. For statistical analysis, the t-test was used when applicable.

The dimensions of the pre-Golgi intermediates were estimated on series of consecutive thin sections. For this, each photographical negative from the respective series of sections was scanned and a drawing of its membrane contours was made manually. All drawings were positioned and overlayed and the dimension of the pre-Golgi intermediates were estimated. Among the serial sections, the largest profile of a pre-Golgi intermediate was determined and its maximum and minimum diameter measured. Their average was taken to represent the dimension of the pre-Golgi intermediate.

Immunofluorescence

Cells grown on coverslips were fixed with 3% formaldehyde in Hanks balanced salt solution for 30 min at initially 37°C, rinsed with PBS, amidinated with 50 mM NH_4Cl in PBS and permeabilized with 0.15% saponin in PBS containing 1% BSA for 15 min. Afterwards, they were simultaneously incubated with mouse monoclonal anti-ERGIC-53 and guinea pig anti-C-peptide antibodies diluted with 0.5% saponin in PBS containing 0.1% BSA for 2 h at ambient temperature, rinsed with PBS containing 0.1% BSA and simultaneously incubated with RedX-conjugated Fab goat anti-mouse IgG and Alexa488-conjugated goat anti-guinea pig IgG antibodies diluted with PBS containing 0.1% BSA for 1 h at ambient temperature. After Moviol embedding, cover slips were inspected by epifluorescence using a Zeiss Axioplan microscope equipped with a digital camera (Axiocam, Zeiss, Oberkochen, Germany). Pictures were acquired using a ×63 (1.4) objective.

Immunoelectron microscopy

For immunogold labeling of ultrathin frozen sections, monolayer CHO cell cultures were fixed in 2% paraformaldehyde and 0.1% glutaraldehyde for 30 min at initially 37°C, washed with several changes of PBS, immersed with PBS containing 50 mM NH_4Cl for 30 min and stored in PBS. Cells were mechanically removed with a rubber policeman, pelleted by centrifugation and enclosed in 2% low melting Agarose. Small pieces of Agarose containing the cells were immersed in 2 M sucrose containing 15% polyvinol pyrrolidone (10 kD), mounted on aluminum pins, frozen and stored in liquid nitrogen. Frozen ultrathin sections were prepared according to Tokuyasu (1978, 1980b) using a Reichert Ultracut S ultramicrotome equipped with a Reichert FCS cryochamber, picked up on nickel grids and stored overnight on gelatin at 4°C. Prior to immunolabeling, gelatin was liquefied at 37°C, the grids removed and washed by floating them on droplets of PBS. For immunolabeling, grids with the attached thin frozen sections were conditioned on droplets of PBS containing 1% milk and 0.01% Triton X-100 for 10 min at ambient temperature. Grids were then transferred to droplets of diluted monoclonal anti-proinsulin antibody for 14 h at 4°C, rinsed on droplets of distilled water, incubated with affinity-purified rabbit anti-mouse IgG antibodies (10 µg/ml, 1 h, and ambient temperature) followed by rinses and 8 nm protein A-gold ($OD_{525\ nm}$ = 0.06) for 1 h at ambient temperature (Roth et al. 1978). Finally, grids were rinsed in PBS, fixed with 2% glutaraldehyde in PBS for 10-20 min, rinsed with PBS and distilled water, and embedded and stained with methylcellulose and uranyl acetate according to Tokuyasu (1978, 1980a). For double immunogold labeling, sections were simultaneously incubated with diluted mouse monoclonal anti-proinsulin antibodies and rabbit anti-β COP antibodies

Table 1 Morphometric evaluation of endoplasmic reticulum, pre-Golgi intermediates, and Golgi apparatus in CHO Ins2 cells

	CHO $Ins2^{wt}$	CHO $Ins2^{C96Y}$	C96Y/wt	*P*
RER, N	2.70 ± 0.02[a]	1.76 ± 0.02[a]	0.65	<0.01
RER, D	0.18 ± 0.08	0.23 ± 0.08	1.28	–
pGI-P	0.21 ± 0.09	2.14 ± 0.26	10.20	<0.001
pGI-G	1.10 ± 0.20	3.10 ± 0.31	2.82	<0.001
pGI-T	0.39 ± 0.92	4.07 ± 2.84	10.44	<0.001
pGI-VT	0.91 ± 1.40	1.25 ± 1.54	1.37	–
Golgi	0.68 ± 1.21	2.00 ± 1.87	2.94	<0.001
Mit	4.78 ± 3.16	4.95 ± 2.89	1.04	–

Based on the evaluation of randomly taken photographs from 20 cells each from three different Epon blocks, for details see Materials and methods

RER, N rough endoplasmic reticulum, *RER, D* dilated rough endoplasmic reticulum, *pGI-G* Golgi associated pre-Golgi intermediates, *pGI-P* not Golgi associated pre-Golgi intermediates, *pGI-T* tubular regions of pre-Golgi intermediates, *pGI-VT* vesicular tubular regions of pre-Golgi intermediates, *Mit* mitochondria

[a] Mean ± SE × 10^{-2} of volume density

followed by rinses and simultaneous incubation with 6 nm goat anti-mouse IgG and 12 nm goat anti-rabbit IgG.

Epon ultrathin sections from aldehyde-OsO_4 fixed cells were mounted on nickel grids, placed on droplets of freshly prepared 1% aqueous periodic acid for 8 min at ambient temperature (Roth et al. 2000) and rinsed by passing them over a series of droplets of distilled water. Sections were conditioned with PBS containing 1% BSA, 0.01% Triton X-100 and 0.01% Tween 20 and transferred to guinea pig anti-rat C-peptide antibodies (250-fold diluted) for 2 h.

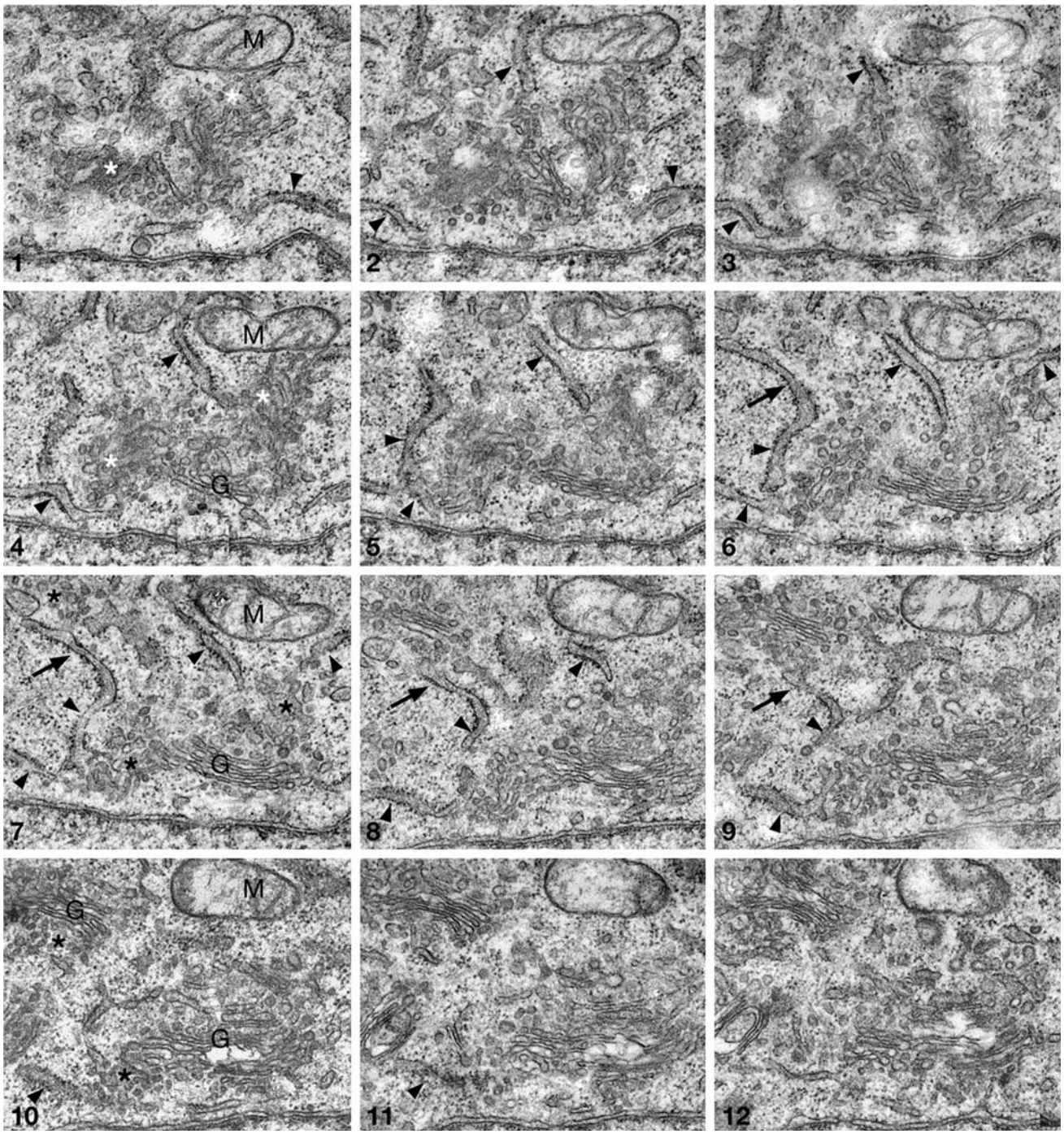

Fig. 1 Series of consecutive ultrathin sections from CHO Ins2^{wt} cells. The spatial relationship between transitional elements of the rough ER (*arrowheads*) and their budding profiles, Golgi-associated pre-Golgi intermediates (*asterisks*), and Golgi apparatus cisternal stacks (*G*) can be only fully appreciated upon serial section analysis. Obviously, several transitional elements of rough ER and pre-Golgi intermediates are associated with a single Golgi cisternal stack. Furthermore, a single ER cisterna can form two exit sites with budding profiles for two distinct Golgi cisternal stacks (arrow in sections 6–9). *M* mitochondrium (magnification ×30,500)

Following rinses with buffer, grids were incubated with 8 nm protein A-gold complexes for 1 h. Finally, thin sections were contrasted with uranyl and lead acetate.

Results

Expression of mutant Ins2^{C96Y} in CHO cells affects the structure of pre-Golgi intermediates but not of the ER

The CHO cell lines analyzed here have been studied previously with regard to the secretion of proinsulin 2 (Wang et al. 1999). Although CHO Ins2^{wt} cells were reported to contain and secrete proinsulin, the mutant Ins2^{C96Y} proinsulin was found to accumulate intracellularly. In the present study, we found that the volume density of the rough ER was significantly decreased in CHO Ins2^{C96Y} cells as compared to CHO Ins2^{wt} cells (Table 1). However, no significant difference was detected in regard to dilated portions of the rough ER due to the large variation (Table 1). In CHO Ins2^{wt} or CHO Ins2^{C96Y} cells, the pre-Golgi intermediates associated with the Golgi apparatus or in the periphery of the cells consisted of transitional elements of the rough ER and of associated vesiculo-tubular clusters as deduced from the analysis of series of consecutive ultrathin sections (Figs. 1, 2, 3, 4). Their structural organization corresponded basically to the one reported for other cell types (Bannykh and Balch 1997; Fan et al. 2003; Farquhar and Hauri 1997; Hauri et al. 2000; Palade 1975; Saraste and Svensson 1991; Zuber et al. 2004). Although the vesiculo-tubular clusters could be followed through more than ten serial sections, particularly in CHO Ins2^{C96Y} cells, the budding zone of the transitional ER was only observed in one or two sections. Furthermore, a single cisterna of the rough ER could exhibit two separate budding zones feeding into distinct cisternal stacks (Fig. 1). In CHO Ins2^{wt} cells, the tubular structures had an average diameter of 36 nm (range 12–84 nm) and in CHO Ins2^{C96Y} cells of 46 nm (range 20–88 nm). As observed previously for pancreatic β-cells of Akita and control mice (Fan et al. 2003; Zuber et al. 2004), the tubules in CHO Ins2^{wt} and in CHO Ins2^{C96Y} cells were always closely related but discrete from transitional elements of the rough ER (Figs. 1, 2). The comparative analysis of the volume density of pre-Golgi intermediates revealed striking differences with a significant increase in CHO Ins2^{C96Y} cells (Table 1; Figs. 3, 4). The volume density of Golgi-associated pre-Golgi intermediates was approximately threefold increased and that of peripheral pre-Golgi intermediates about tenfold. The average diameter of both Golgi-associated and peripheral pre-Golgi intermediates was twofold increased in CHO Ins2^{C96Y} cells (Table 2). A detailed analysis furthermore demonstrated that the increase in

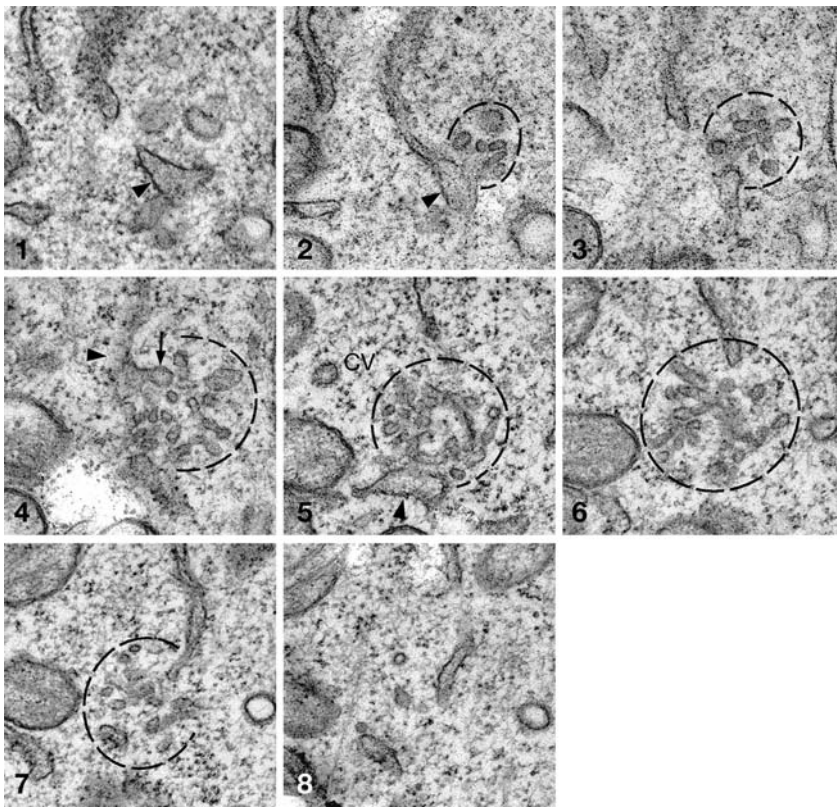

Fig. 2 Serial section analysis of a peripheral pre-Golgi intermediate in CHO Ins2^{wt} cells. The transitional element of the rough ER is marked by an *arrowhead* and the vesiculo-tubular cluster by a *broken line*. The *arrow* in section 4 points to a budding profile. *cv* clathrin-coated vesicle (magnification ×45,000)

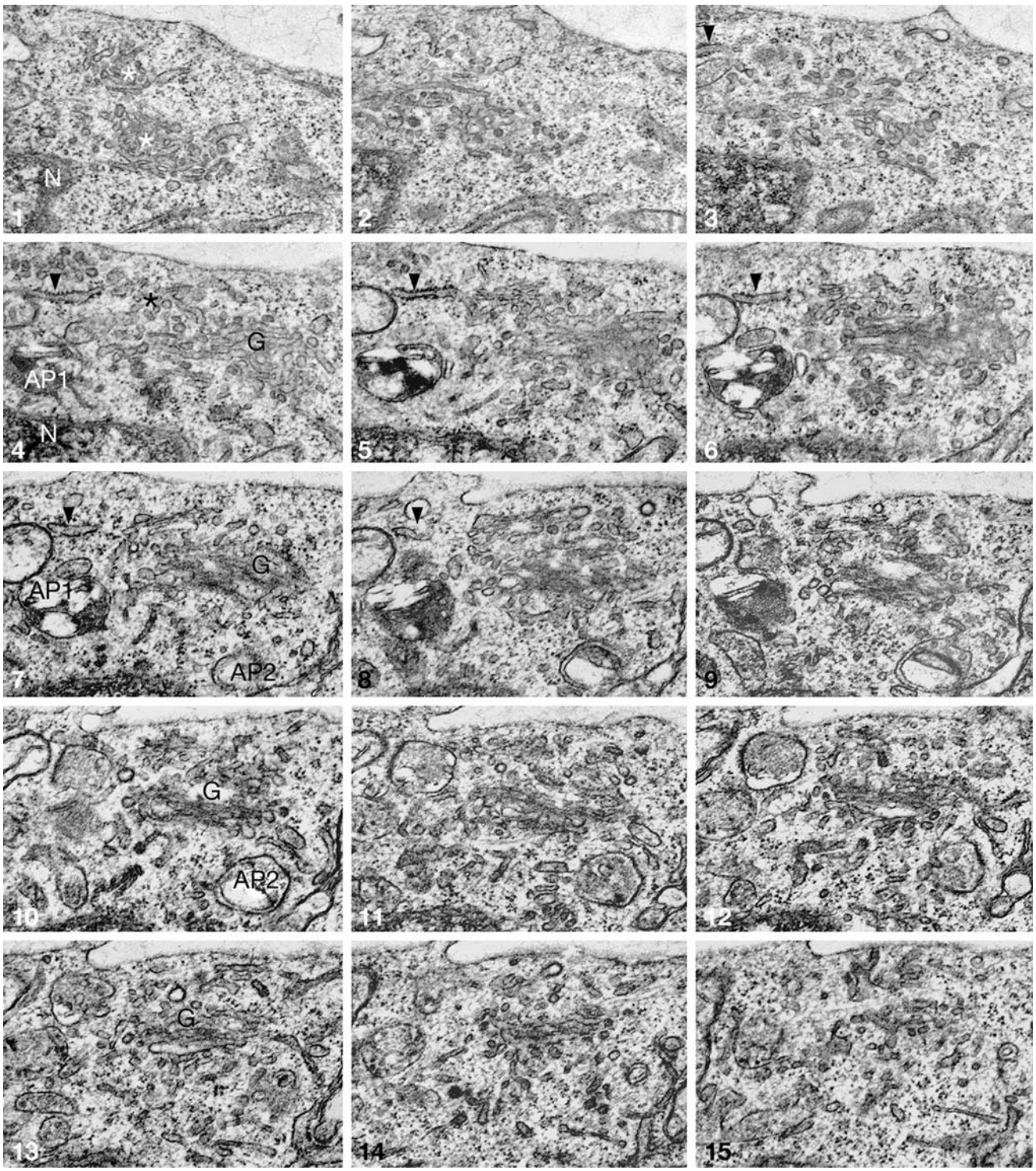

Fig. 3 Series of 15 consecutive ultrathin sections out of 24 serial sections from CHO Ins2^{C96Y} cells showing a Golgi-associated pre-Golgi intermediate (*asterisks*). The numerous tubules are obvious. *Arrowheads*: transitional element of rough ER. *G* Golgi apparatus, *N* nucleus, *AP1*, *AP2* autophagosomes (magnification ×33,500)

volume density of pre-Golgi intermediates was due to tubules (Table 1). As already estimated for pancreatic β-cells of Akita mice (Zuber et al. 2004), an about threefold increase in volume density of the Golgi apparatus of CHO Ins2^{C96Y} cells was found (Table 1). On the average, the cisternal stack of CHO Ins2^{C96Y} cell Golgi apparatus contained 1–2 additional cisternae as compared to CHO Ins2^{wt} cells (Table 3). However, the profile area

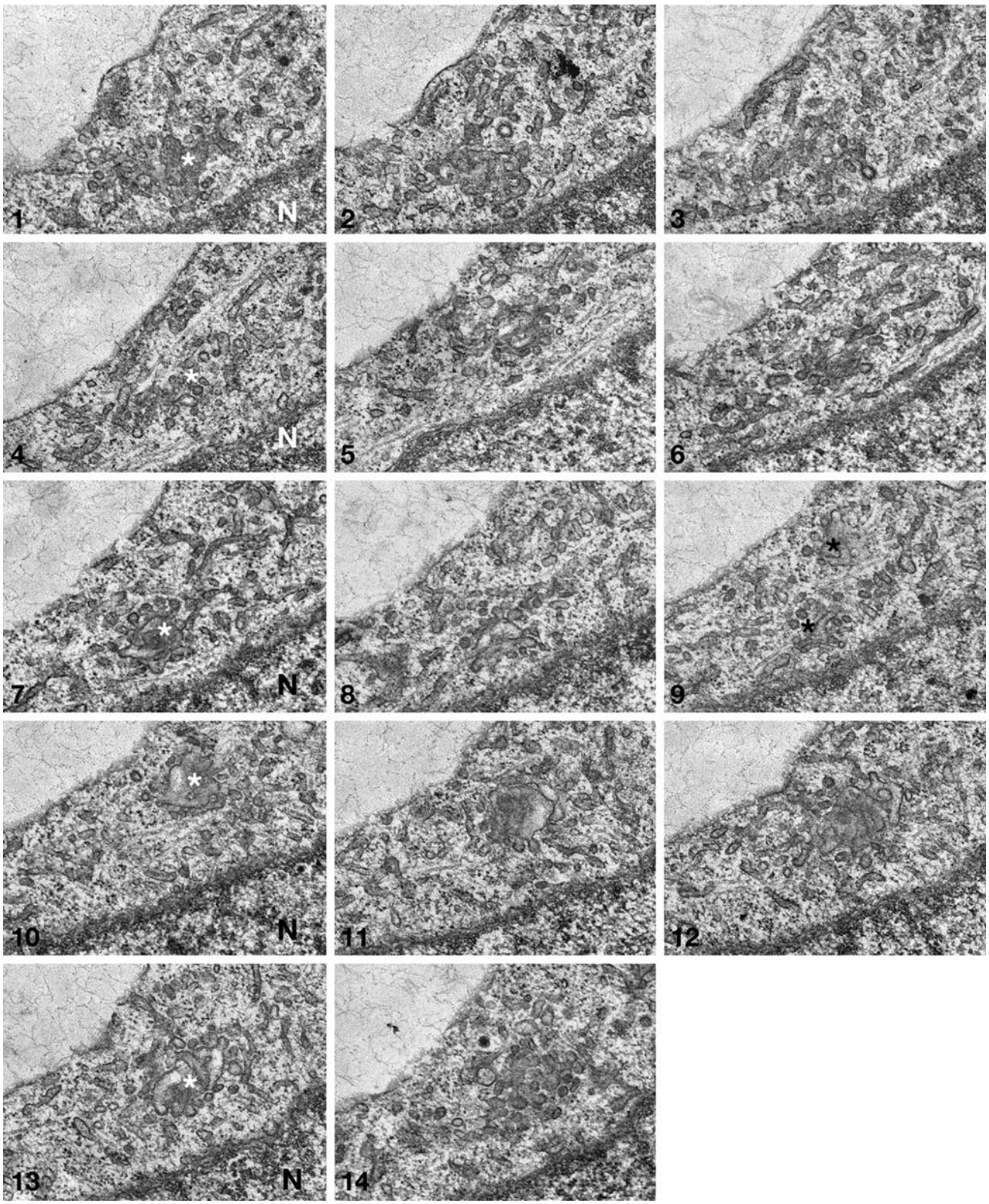

Fig. 4 Series of 14 consecutive ultrathin sections out of 24 serial sections from CHO Ins2^{C96Y} cells showing two peripheral pre-Golgi intermediates (*asterisks*). Note the abundant tubules and the pleomorphic structure exhibiting numerous budding profiles (sections 7 and 8). *N* nucleus (magnification ×30,000)

Table 2 Dimension of pre-Golgi intermediates in CHO Ins2 cells

Numbers	CHO Ins2^{wt}			CHO Ins2^{C96Y}		
	D_{MA} (μm)	D_{MI} (μm)	D_{AV} (μm)	D_{MA} (μm)	D_{MI} (μm)	D_{AV} (μm)
1	1.0	0.6	0.8	2.4	1.5	2.0
2	1.0	0.9	1.0	1.5	1.0	1.3
3	0.8	0.3	0.6	2.4	1.3	1.9
4	0.9	0.4	0.7	1.0	1.0	1.0
5	0.8	0.5	0.7	1.0	0.8	0.9
6	1.0	1.0	1.0	2.6	1.6	2.1[a]
7	0.5	0.3	0.4[a]	0.7	0.6	0.7[a]
8	0.6	0.2	0.4[a]	1.9	1.5	1.7[a]
9	0.6	0.4	0.5[a]	1.0	0.9	1.0[a]
10	1.1	0.8	0.9[a]	1.7	1.0	1.4[a]
Mean ± SE of D_{AV}			0.7 ± 0.06			1.40 ± 0.16

Based on the evaluation of series of consecutive ultrathin sections

D_{MA} maximal diameter, D_{MI} minimal diameter, D_{AV} average diameter

[a] Not Golgi associated pre-Golgi intermediates

of the entire stack and that of the first and of the second *cis* Golgi apparatus cisternae were the same in CHO Ins2^{wt} and CHO Ins2^{C96Y} cells (Table 3). The volume density of mitochondria was not different between CHO Ins2^{wt} and CHO Ins2^{C96Y} cells (Table 1).

Distribution of Ins2 in CHO cells

By double immunofluorescence, proinsulin in CHO Ins2^{C96Y} cells was detectable in the nuclear envelope, throughout the ER and in ERGIC-53 positive structures (Fig. 5). By immunogold labeling of ultrathin frozen sections of the human adenocarcinoma cell line Caco-2, the monoclonal anti-ERGIC-53 antibody was originally described to label a tubulovesicular compartment near the cis side of the Golgi apparatus, including the first cis-cisterna itself (Schweizer et al. 1988). In ultrathin frozen sections prepared from CHO Ins2^{C96Y} cells, immunogold labeling for proinsulin was observed over the nuclear envelope, throughout the ER and in the pre-Golgi intermediates (alias

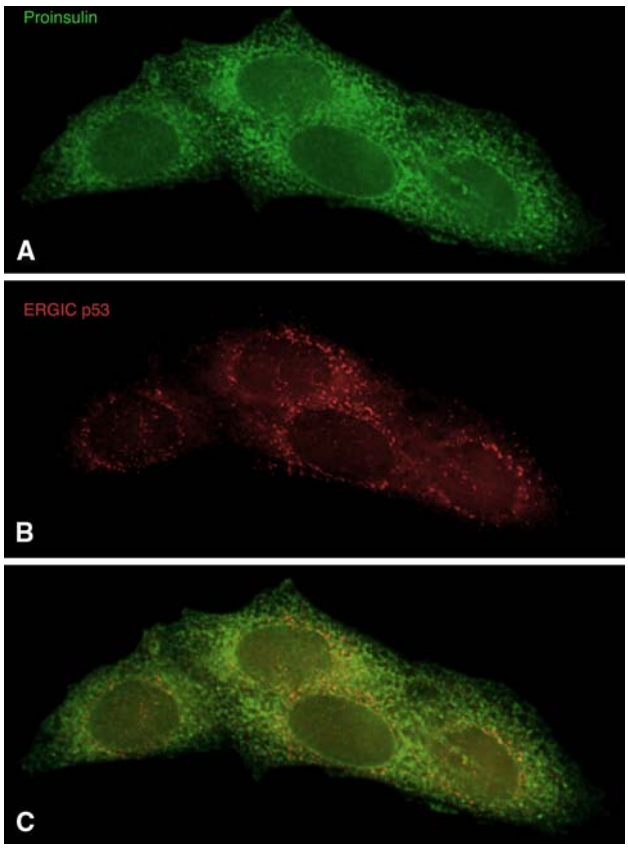

Fig. 5 Double immunofluorescence for proinsulin and ERGIC-53, CHO Ins2^{C96Y} cells. **a** Proinsulin immunoreactivity as detected with the anti-C-peptide antibody is observed in nuclear envelope, throughout the ER and ERGIC-53 positive perinuclear structures. **b** ERGIC-53 immunofluorescence exhibites the typical perinuclear pattern. **c** In the overlay, proinsulin and ERGIC-53 labeling overlap (magnification ×1,000)

ERGIC-53), whereas the Golgi apparatus cisternal stack was consistently unlabeled (Fig. 6). Proinsulin immunolabeling was not detectable in non-transfected cells or when the monoclonal proinsulin antibody was omitted (not shown). In CHO Ins2^{wt} cells, only negligible labeling for proinsulin was detectable (not shown), which would be in agreement with the biochemical data on its rapid secretion (Wang et al. 1999). Although by double immunogold

Table 3 Morphometric evaluation of the Golgi apparatus in CHO Ins2 cells

	CHO Ins2^{wt}	CHO Ins2^{C96Y}	*P*
Number of cisternae per stack	5.050 ± 1.234	6.650 ± 2.477	<0.01
Profile area of cisternal stack	0.112 ± 0.031[a]	0.139 ± 0.083[a]	–
Profile area of first *cis* cisterna	0.011 ± 0.005[a]	0.014 ± 0.006[a]	–
Profile area of second *cis* cisterna	0.013 ± 0.007[a]	0.015 ± 0.005[a]	–

Based on the evaluation of 30 Golgi apparatus

[a] Mean ± SE in μm^2

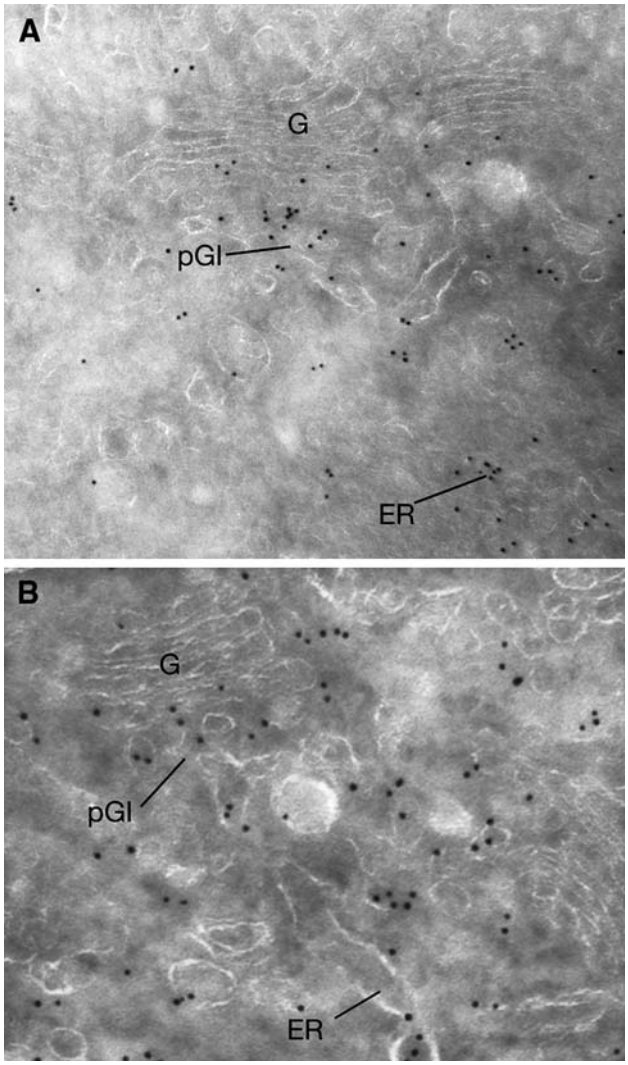

Fig. 6 Ultrathin frozen sections from CHO Ins2^{C96Y} cells, immunogold labeling for proinsulin. **a**, **b** Gold particles are present over the ER and Golgi-associated pre-Golgi intermediates (*pGI*). The Golgi apparatus cisternal stack (*G*) does not exhibit immunolabeling (magnification ×69,000 **a**, ×88,000 **b**)

labeling, proinsulin and β-COP were both present in pre-Golgi intermediates, no colocalization was observed (Fig. 7). Immunogold labeling for β-COP in different cell types has shown a rather wide distribution including the ER-Golgi boundary, Golgi cisternal buds and vesicles at the lateral rims as well as membrane of the trans-Golgi network (Griffiths et al. 1995; Orci et al. 1994).

Proteasome inhibition causes aggresome formation in Ins2 expressing CHO cells

For proteasome inhibition, cells were grown in the presence of lactacystin or MG 132. This short time exposure to the proteasome inhibitors resulted in the formation of pericentriolar located highly electron dense

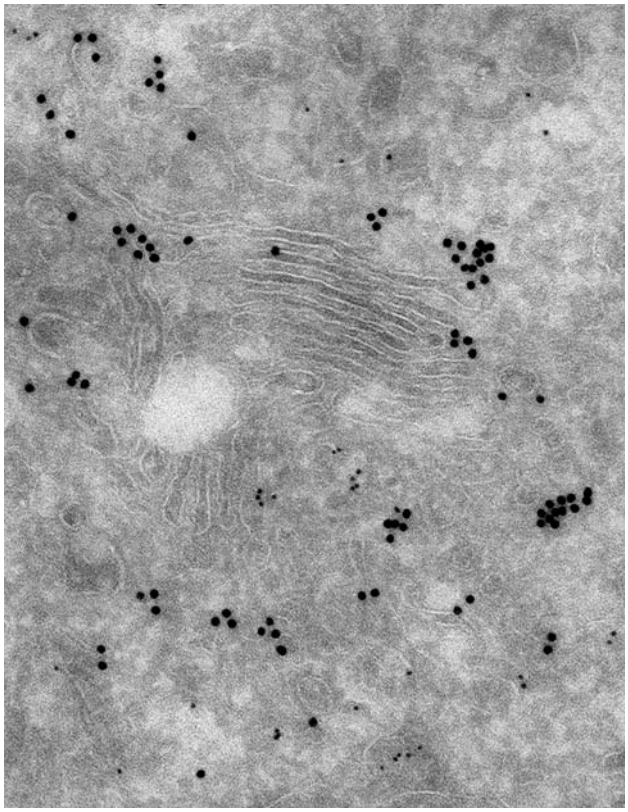

Fig. 7 Ultrathin frozen sections from CHO Ins2^{C96Y} cells, double immunogold labeling for proinsulin and β-COP. Immunogold labeling for proinsulin (*small gold particles*) and β-COP (*large gold particles*) is detected over different structures (magnification ×70,000)

clumps (aggresomes) in CHO Ins2^{C96Y} cells which were surrounded by intermediate filaments most probably representing vimentin fibers (Fig. 8). The electron dense material was reactive with an anti- C-peptide antibody when ultrathin sections of Epon embedded cells that had been subjected to antigen retrieval were investigated (Fig. 8b).

Discussion

In continuation of our previous analysis of pancreatic β-cells in Akita mice (Fan et al. 2003; Zuber et al. 2004), we have studied CHO cells expressing singly either Ins2^{wt} or Ins2^{C96Y}. The most striking change was the significantly increased volume density of the pre-Golgi intermediates in CHO Ins2^{C96Y} cells, which was principally due an increase of its tubular elements. The enlarged pre-Golgi intermediates and the ER of CHO Ins2^{C96Y} cells were positive for proinsulin, which was not detectable in the Golgi cisternal stack. Treatment of CHO Ins2^{C96Y} cells with proteasome inhibitors resulted in the formation of typical aggresomes.

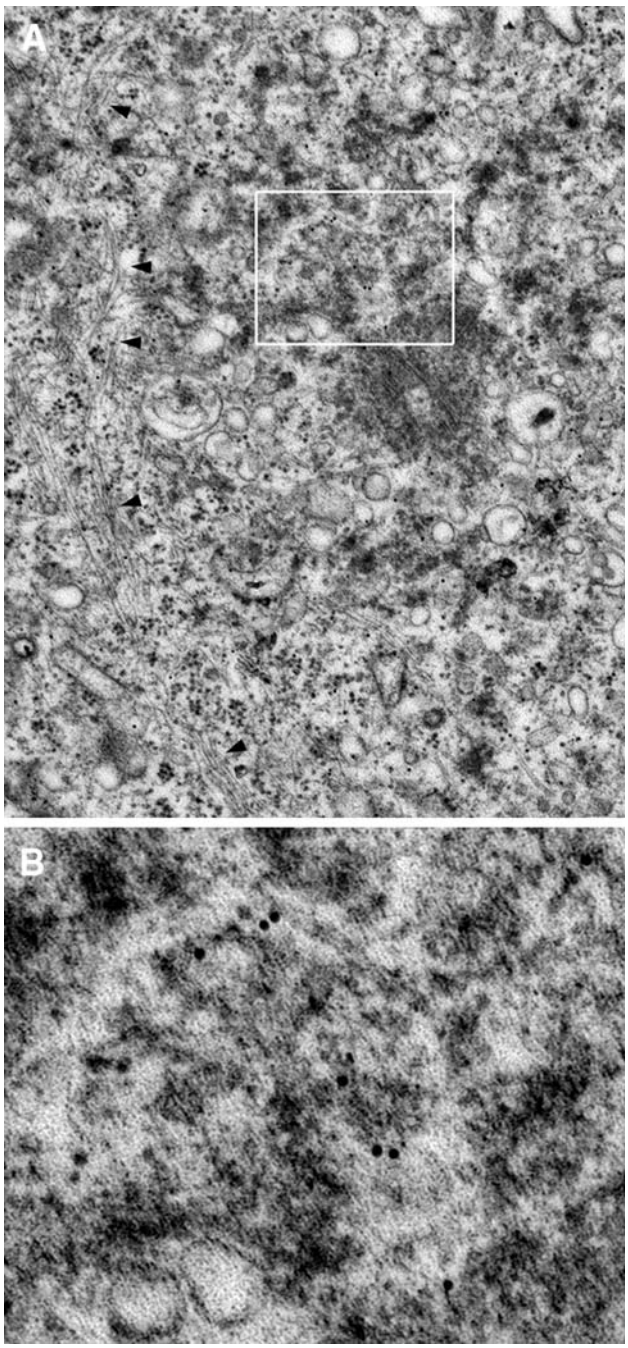

Fig. 8 CHO $Ins2^{C96Y}$ cells treated with lactacystin for 4 h. **a** Pericentriolar clumps of electron dense material partially surrounded by a bundle intermediate filaments are obvious (*arrowheads*). **b** Enlargement of the marked field in **a**. The electron dense material is labeled with an antibody directed against C-peptide (magnification ×24,000 **a**, ×73,000 **b**)

In contrast to pancreatic β-cells in Akita mice which simultaneously synthesize wild type insulin 1 and 2 and mutant C96Y proinsulin 2, CHO $Ins2^{C96Y}$ cells exhibit somewhat different ultrastructural changes. Although the volume density of narrow rough ER was decreased in both Akita β-cells and transfected CHO cells, the dilated rough ER was not significantly increased in CHO $Ins2^{C96Y}$ cells. This probably is related to the efficient ubiquitination and proteasomal degradation of $Ins2^{C96Y}$ as observed in transfected COS7 cells (Allen et al. 2004). Treatment of COS7 $Ins2^{C96Y}$ cells with the proteasome inhibitor MG 132 resulted in increased steady state levels of mutant insulin and this was influenced by HRD1-mediated ubiquitination. The data obtained on $Ins2^{C96Y}$-expressing COS7 cells suggest that the mutant insulin 2 becomes efficiently degraded in a proteasome-dependent manner. This is also supported by our electron microscopic analysis of CHO $Ins2^{C96Y}$ cells in which the formation of proinsulin-reactive aggresomes could be observed following inhibition of proteasomes by MG 132 or lactacystin. We also observed the formation of aggresomes in CHO $Ins2^{wt}$ cells, but they were smaller and less numerous. If this is related to the missing conversion of wild type proinsulin to insulin in transfected CHO cells (Wang et al. 1999) remains to be elucidated. In this context, it is interesting to note that the fate of mutant, non-convertable proinsulin seems to depend on the cell type it is expressed. A non-convertable $proinsulin^{R32G/K64T}$ was sorted and secreted as efficiently as wild type proinsulin in primary rat pancreatic β-cells (Halban and Irminger 2003). Nonetheless, as shown in pulse-chase experiments, initially about 20% of the mutant proinsulin was proteasomally degraded which is indicative of its recognition by the protein quality control.

The present observations confirm and extend our previous ones on pancreatic β-cells of Akita mice (Zuber et al. 2004) that mutant $Ins2^{C96Y}$ accumulates in enlarged pre-Golgi intermediates. In both pancreatic β-cells and in transfected CHO cells, it was the tubular elements which caused their enlarged dimensions and higher volume density. Although the average diameter of pre-Golgi intermediates of Akita mice pancreatic β-cells (0.67 ± 0.04 μm) and transfected CHO cells (1.40 ± 0.16 μm) was different, in both cell types there dimensions were about twofold enlarged as compared to the controls. In view of the present data, the dimensional change of the pre-Golgi intermediates appears to be primarily due to mutant Ins^{C96Y}. The reason for the higher increase of volume density of peripheral pre-Golgi intermediates as compared to Golgi-associated ones in CHO $Ins2^{C96Y}$ cells, which actually reflects an numerical increase, remains enigmatic. Taken together, the entry and/or accumulation of misfolded proteins seems to affect the structural organization of the pre-Golgi intermediates (Gilbert et al. 1998; Hsu et al. 1991; Moolenaar et al. 1997; Raposo et al. 1995; Schweizer et al. 1990; Vanslyke et al. 2000).

We also observed a significant increase of volume density of the Golgi apparatus in the presence of $Ins2^{C967Y}$ (Zuber et al. 2004 and present study). We can now exclude

that this might be related to coexistence of wild type insulin 1 and 2 and of mutant proinsulin. Singly $Ins2^{C96Y}$ expressing CHO cells showed a similar threefold increase in Golgi apparatus volume density as did Akita mice pancreatic β-cells. However, proinsulin was undetectable in the Golgi cisternal stack of transfected CHO cells. If this reflects absence of proinsulin or is indication of its fast entry and retrograde transport to the ER remains to be solved. It has been proposed that misfolded proteins in order to become eventually degraded will undergo COPII-mediated transport to the Golgi apparatus and subsequent retrieval via retrograde transport (Caldwell et al. 2001; Vashist et al. 2001; Vashist and Ng 2004).

The possible involvement of the induced tubules of the pre-Golgi intermediates in the retrotranslocation of $proinsulin^{C96Y}$ cannot be answered by the present study. In contrast to the many details known about the ERAD of misfolded glycoproteins, rather little is known about the degradation of misfolded non-glycosylated proteins (Carvalho et al. 2006; Denic et al. 2006; Ismail and Ng 2006). The misfolded Hong Kong variant of α1-antitrypsin, which is detectable in both the ER and the pre-Golgi intermediates (Torossi et al. 2006), has been shown to exit the ER via EDEM1-positive vesicles (Zuber et al. 2007). This novel vesicular transport pathway from the ER, however, does not involve transitional ER and vesiculotubular clusters of pre-Golgi intermediates.

Acknowledgments We would like to thank Dr. H.-P. Hauri (Biozentrum, University of Basel, Switzerland), Dr. O. Madsen (Hagedorn Research Laboratory, Gentofte, Denmark), and Dr. R. Pepperkok (EMBL, Heidelberg, Germany) for antibodies and Dr. T. Izumi (Gunma University, Maebashi, Gunma, Japan) for cell lines. This work was supported by the Swiss National Science Foundation and the Canton of Zurich.

References

Alanen A, Pira U, Lassila O, Roth J, Franklin R (1985) Mott cells are plasma cells defective in immunoglobulin secretion. Eur J Immunol 15:235–242

Allen JR, Nguyen LX, Sargent KE, Lipson KL, Hackett A, Urano F (2004) High ER stress in beta-cells stimulates intracellular degradation of misfolded insulin. Biochem Biophys Res Commun 324:166–170

Aridor M, Hannan LA (2002) Traffic jams II: an update of diseases of intracellular transport. Traffic 3:781–790

Bannykh SI, Balch WE (1997) Membrane dynamics at the endoplasmic reticulum-Golgi interface. J Cell Biol 138:1–4

Barral JM, Broadley SA, Schaffar G, Hartl FU (2004) Roles of molecular chaperones in protein misfolding diseases. Semin Cell Dev Biol 15:17–29

Caldwell SR, Hill KJ, Cooper AA (2001) Degradation of endoplasmic reticulum (ER) quality control substrates requires transport between the ER and Golgi. J Biol Chem 276:23296–23303

Carvalho P, Goder V, Rapoport TA (2006) Distinct ubiquitin-ligase complexes define convergent pathways for the degradation of ER proteins. Cell 126:361–373

Denic V, Quan EM, Weissman JS (2006) A luminal surveillance complex that selects misfolded glycoproteins for ER-associated degradation. Cell 126:349–359

Ellgaard L, Helenius A (2003) Quality control in the endoplasmic reticulum. Nat Rev Mol Cell Biol 4:181–191

Fabunmi RP, Wigley WC, Thomas PJ, DeMartino GN (2000) Activity and regulation of the centrosome-associated proteasome. J Biol Chem 275:409–413

Fan JY, Roth J, Zuber C (2003) Ultrastructural analysis of transitional endoplasmic reticulum and pre-Golgi intermediates: a highway for cars and trucks. Histochem Cell Biol 120:455–463

Farquhar M, Hauri H-P (1997) Protein sorting and vesicular traffic in the Golgi apparatus. In: Berger E, Roth J (eds) The Golgi apparatus. Birkhäuser Verlag, Basel, Boston, Berlin, pp 63–129

Garcia-Mata R, Gao YS, Sztul E (2002) Hassles with taking out the garbage: aggravating aggresomes. Traffic 3:388–396

Gilbert A, Jadot M, Leontieva E, Wattiaux D-C-S, Wattiaux R (1998) Delta F508 CFTR localizes in the endoplasmic reticulum-Golgi intermediate compartment in cystic fibrosis cells. Exp Cell Res 242:144–152

Griffiths G, Pepperkok R, Locker JK, Kreis TE (1995) Immunocytochemical localization of beta-COP to the ER-Golgi boundary and the TGN. J Cell Sci 108:2839–2856

Halban PA, Irminger JC (2003) Mutant proinsulin that cannot be converted is secreted efficiently from primary rat beta-cells via the regulated pathway. Mol Biol Cell 14:1195–1203

Harding HP, Ron D (2002) Endoplasmic reticulum stress and the development of diabetes: a review. Diabetes 51(Suppl 3):S455–S461

Hauri HP, Kappeler F, Andersson H, Appenzeller C (2000) ERGIC-53 and traffic in the secretory pathway. J Cell Sci 113:587–596

Hirano K, Zuber C, Roth J, Ziak M (2003) The proteasome is involved in the degradation of different aquaporin-2 mutants causing nephrogenic diabetes insipidus. Am J Pathol 163:111–120

Hsu VW, Yuan LC, Nuchtern JG, Lippincott-Schwartz J, Hammerling GJ, Klausner RD (1991) A recycling pathway between the endoplasmic reticulum and the Golgi apparatus for retention of unassembled MHC class I molecules. Nature 352:441–444

Ismail N, Ng DT (2006) Have you HRD? Understanding ERAD is DOAble! Cell 126:237–239

Johnston JA, Ward CL, Kopito RR (1998) Aggresomes: a cellular response to misfolded proteins. J Cell Biol 143:1883–1898

Kayo T, Koizumi A (1998) Mapping of murine diabetogenic gene Mody on chromosome 7 at D7Mit258 and its involvement in pancreatic islet and b cell development during the perinatal period. J Clin Invest 101:2112–2118

Kim PS, Arvan P (1998) Endocrinopathies in the family of endoplasmic reticulum (ER) storage diseases: disorders of protein trafficking and the role of ER molecular chaperones. Endocr Rev 19:173–202

Kopito RR, Sitia R (2000) Aggresomes and Russell bodies. Symptoms of cellular indigestion? EMBO Rep 1:225–231

Lucocq J, Baschong W (1986) Preparation of protein colloidal gold complexes in the presence of commonly used buffers. Eur J Cell Biol 42:332–337

Lukacs GL, Mohamed A, Kartner N, Chang XB, Riordan JR, Grinstein S (1994) Conformational maturation of CFTR but not its mutant counterpart (delta F508) occurs in the endoplasmic reticulum and requires ATP. Embo J 13:6076–6086

Madsen OD, Frank BH, Steiner DF (1984) Human proinsulin-specific antigenic determinants identified by monoclonal antibodies. Diabetes 33:1012–1016

Mattioli L, Anelli T, Fagioli C, Tacchetti C, Sitia R, Valetti C (2006) ER storage diseases: a role for ERGIC-53 in controlling the formation and shape of Russell bodies. J Cell Sci 119:2532–2541

McNaught KSP, Shashidharan P, Perl DP, Jenner P, Olanow CW (2002) Aggresome-related biogenesis of Lewy bodies. Eur J Neurosci 16:2136–2148

MedeirosNeto G, Kim PS, Yoo SE, Vono J, Targovnik HM, Camargo R, Hossain SA, Arvan P (1996) Congenital hypothyroid goiter with deficient thyroglobulin–identification of an endoplasmic reticulum storage disease with induction of molecular chaperones. J Clin Invest 98:2838–2844

Meusser B, Hirsch C, Jarosch E, Sommer T (2005) ERAD: the long road to destruction. Nat Cell Biol 7:766–772

Moolenaar CEC, Ouwendijk J, Wittpoth M, Wisselaar HA, Hauri HP, Ginsel LA, Naim HY, Fransen JAM (1997) A mutation in a highly conserved region in brush-border sucrase-isomaltase and lysosomal alpha-glucosidase results in Golgi retention. J Cell Sci 110:557–567

Naim H, Roth J, Sterch E, Lentze M, Milla P, Schmitz J, Hauri H (1988) Sucrase-isomaltase deficiency in humans. Different mutations disrupt intracellular transport, processing, and function of an intestinal brush border enzyme. J Clin Invest 82:667–679

Orci L, Perrelet A, Ravazzola M, Amherdt M, Rothman JE, Schekman R (1994) Coatomer-rich endoplasmic reticulum. Proc Natl Acad Sci USA 91:11924–11928

Oyadomari S, Araki E, Mori M (2002a) Endoplasmic reticulum stress-mediated apoptosis in pancreatic beta-cells. Apoptosis 7:335–345

Oyadomari S, Koizumi A, Takeda K, Gotoh T, Akira S, Araki E, Mori M (2002b) Targeted disruption of the Chop gene delays endoplasmic reticulum stress-mediated diabetes. J Clin Invest 109:525–532

Palade G (1975) Intracellular aspects of the process of protein biosynthesis. Science 189:347–358

Pepperkok R, Scheel J, Horstmann H, Hauri HP, Griffiths G, Kreis TE (1993) beta-COP Is essential for biosynthetic membrane transport from the endoplasmic reticulum to the Golgi complex Invivo. Cell 74:71–82

Petäjä-Repo U, Hogue M, Laperrière A, Walkers P, Bouvier M (2000) Export from the endoplasmic reticulum represents the limiting step in the maturation and cell surface expression of the human d opiod receptor. J Biol Chem 275:13727–13736

Raposo G, van S-HM, Leijendekker R, Geuze HJ, Ploegh HL (1995) Misfolded major histocompatibility complex class I molecules accumulate in an expanded ER-Golgi intermediate compartment. J Cell Biol 131:1403–1419

Roth J, Bendayan M, Orci L (1978) Ultrastructural localization of intracellular antigens by the use of protein A-gold complex. J Histochem Cytochem 26:1074–1081

Roth J, Ziak M, Guhl B (2000) Non-heating antigen retrieval techniques for light and electron microscopic immunolabeling. In: Taylor CR, Shi S-R (eds) Antigen retrieval technique: a revolutionary approach to routine immunohistochemistry. Eaton Publishing, Natick, MA, pp 275–285

Roth J (2002) Protein N-glycosylation along the secretory pathway: relationship to organelle topography and function, protein quality control, and cell interactions. Chem Rev 102:285–303

Saraste J, Svensson K (1991) Distribution of intermediate elements operating in ER to Golgi transport. J Cell Sci 100:415–430

Schweizer A, Fransen J, Bächi T, Ginsel L, Hauri H (1988) Identification, by a monoclonal antibody, of a 53 kD protein associated with tubulovescular compartment at the cis-side of the Golgi apparatus. J Cell Biol 107:1643–1653

Schweizer A, Fransen JA, Matter K, Kreis TE, Ginsel L, Hauri HP (1990) Identification of an intermediate compartment involved in protein transport from endoplasmic reticulum to Golgi apparatus. Eur J Cell Biol 53:185–196

Sitia R, Braakman I (2003) Quality control in the endoplasmic reticulum protein factory. Nature 426:891–894

Tamarappoo BK, Verkman AS (1998) Defective aquaporin-2 trafficking in nephrogenic diabetes insipidus and correction by chemical chaperones. J Clin Invest 101:2257–2267

Tokuyasu K (1978) A study of positive staining of ultrathin frozen sections. J Ultrastruct Res 63:287–307

Tokuyasu K (1980a) Immunochemistry on ultrathin frozen sections. Histochem J 12:381–403

Tokuyasu K (1980b) Adsorption staining method for ultrathin frozen sections. In: Bailey G (ed) Proceedings of the 38th meeting of the electron microscopy society of America, Baton Rouge, pp 760–763

Torossi T, Fan JY, Sauter-Etter K, Roth J, Ziak M (2006) Endomannosidase processes oligosaccharides of alpha1-antitrypsin and its naturally occurring genetic variants in the Golgi apparatus. Cell Mol Life Sci 63:1923–1932

Valetti C, Grossi CE, Milstein C, Sitia R (1991) Russell bodies: a general response of secretory cells to synthesis of a mutant immunoglobulin which can neither exit from, nor be degraded in, the endoplasmic reticulum. J Cell Biol 115:983–994

Vanslyke JK, Deschenes SM, Musil LS (2000) Intracellular transport, assembly, and degradation of wild-type and disease-linked mutant gap junction proteins. Mol Biol Cell 11:1933–1946

Vashist S, Kim W, Belden WJ, Spear ED, Barlowe C, Ng DT (2001) Distinct retrieval and retention mechanisms are required for the quality control of endoplasmic reticulum protein folding. J Cell Biol 155:355–368

Vashist S, Ng DT (2004) Misfolded proteins are sorted by a sequential checkpoint mechanism of ER quality control. J Cell Biol 165:41–52

Wang J, Takeuchi T, Tanaka S, Kubo SK, Kayo T, Lu D, Takata K, Koizumi A, Izumi T (1999) A mutation in the insulin 2 gene induces diabetes with severe pancreatic beta-cell dysfunction in the Mody mouse. J Clin Invest 103:27–37

Ward CL, Kopito RR (1994) Intracellular turnover of cystic fibrosis transmembrane conductance regulator. Inefficient processing and rapid degradation of wild-type and mutant proteins. J Biol Chem 269:25710–25718

Weibel E (1979) Stereological methods. 1. Practical methods for biological morphometry: Academic, New York

Wigley WC, Fabunmi RP, Lee MG, Marino CR, Muallem S, DeMartino GN, Thomas PJ (1999) Dynamic association of proteasomal machinery with the centrosome. J Cell Biol 145:481–490

Wojcik C, Schroeter D, Wilk S, Lamprecht J, Paweletz N (1996) Ubiquitin-mediated proteolysis centers in HeLa cells: indication from studies of an inhibitor of the chymotrypsin-like activity of the proteasome. Eur J Cell Biol 71:311–318

Yam GH, Bosshard N, Zuber C, Steinmann B, Roth J (2006) Pharmacological chaperone corrects lysosomal storage in Fabry disease caused by trafficking-incompetent variants. Am J Physiol Cell Physiol 290:C1076–C1082

Yam GH, Gaplovska-Kysela K, Zuber C, Roth J (2007) Aggregated myocilin induces Russell bodies and causes apoptosis: implications for the pathogenesis of myocilin-caused primary open-angle glaucoma. Am J Pathol 170:100–109

Yoshioka M, Kayo T, Ikeda T, Koizumi A (1997) A novel locus, *Mody4*, distal to D7Mit189 on chromosome 7 determines early-onset NIDDM in nonobese C57BL/6J (Akita) mutant mice. Diabetes 46:887–894

Zatloukal K, Stumptner C, Fuchsbichler A, Heid H, Schnoelzer M, Kenner L, Kleinert R, Prinz M, Aguzzi A, Denk H (2002) p62 Is a common component of cytoplasmic inclusions in protein aggregation diseases. Am J Pathol 160:255–263

Zuber C, Fan JY, Guhl B, Roth J (2004) Misfolded proinsulin accumulates in expanded pre-Golgi intermediates and endoplasmic reticulum subdomains in pancreatic beta cells of Akita mice. FASEB J 18:917–919

Zuber C, Cormier JH, Guhl B, Santimaria R, Hebert DN, Roth J (2007) EDEM1 reveals a quality control vesicular transport pathway out of the endoplasmic reticulum not involving the COPII exit sites. Proc Natl Acad Sci USA 104:4407–4412